



OPEN ACCESS

EDITED BY

Mohamed L. Ashour,
Ain Shams University, Egypt

REVIEWED BY

Changan Geng,
Kunming Institute of Botany (CAS),
China
Doaa A Ghareeb,
Alexandria University, Egypt
Olfat Ali Hammam,
Theodor Bilharz Research Institute,
Egypt

*CORRESPONDENCE

Gabriela Rosas Salgado,
gabriela.rosas@uaem.mx,
gabyrosas62@hotmail.com

SPECIALTY SECTION

This article was submitted to Biological Activities of Natural Products, a section of the journal Frontiers in Natural Products

RECEIVED 13 September 2022

ACCEPTED 25 October 2022

PUBLISHED 09 November 2022

CITATION

Alvarado-Ojeda ZA, Coset Mejia A, Arrellin Rosas G, Jiménez-Ferrer JE, Zamilpa A, Trejo-Moreno C, Castro Martínez G, Méndez Martínez M, Cervantes Torres J, Báez Reyes JC, Fragoso G and Rosas Salgado G (2022), Hepatoprotective effect of hydroalcoholic extract from root of *Sechium edule* (Jacq.) Sw. over hepatic injury induced by chronic application of angiotensin II. *Front. Nat. Prod.* 1:1043685. doi: 10.3389/fntpr.2022.1043685

COPYRIGHT

© 2022 Alvarado-Ojeda, Coset Mejia, Arrellin Rosas, Jiménez-Ferrer, Zamilpa, Trejo-Moreno, Castro Martínez, Méndez Martínez, Cervantes Torres, Báez Reyes, Fragoso and Rosas Salgado. This is an open-access article distributed under the terms of the [Creative Commons Attribution License \(CC BY\)](https://creativecommons.org/licenses/by/4.0/). The use, distribution or reproduction in other forums is permitted, provided the original author(s) and the copyright owner(s) are credited and that the original publication in this journal is cited, in accordance with accepted academic practice. No use, distribution or reproduction is permitted which does not comply with these terms.

Hepatoprotective effect of hydroalcoholic extract from root of *Sechium edule* (Jacq.) Sw. over hepatic injury induced by chronic application of angiotensin II

Zimri Azriel Alvarado-Ojeda¹, Alejandro Coset Mejia¹, Gerardo Arrellin Rosas^{1,2}, Jesús Enrique Jiménez-Ferrer³, Alejandro Zamilpa³, Celeste Trejo-Moreno¹, Gabriela Castro Martínez⁴, Marisol Méndez Martínez⁵, Jacquelynne Cervantes Torres⁶, Juan Carlos Báez Reyes⁷, Gladis Fragoso⁶ and Gabriela Rosas Salgado^{1*}

¹Facultad de Medicina, Universidad Autónoma del Estado de Morelos, Cuernavaca, Mexico, ²Facultad de Ciencias de la Salud, Universidad Panamericana, México City, Mexico, ³Laboratorio de Farmacología, Centro de Investigaciones Biomédicas del Sur, Instituto Mexicano del Seguro Social, Xochitepec, Mexico, ⁴División de ciencias Biológicas y de la salud, Universidad Autónoma Metropolitana-Iztapalapa, Iztapalapa, Mexico, ⁵Departamento de Sistemas Biológicos, Universidad Autónoma Metropolitana-Xochimilco, Mexico City, Mexico, ⁶Departamento de Inmunología, Instituto de Investigaciones Biomédicas, Universidad Nacional Autónoma de México, México City, Mexico, ⁷Escuela Nacional Preparatoria No. 1 UNAM, Xochimilco, Mexico

Liver damage is characterized by lipid accumulation in the liver, a prooxidant/proinflammatory state, necrosis, and fibrosis. Given the multifactorial conditions and complexity of the disease and the contribution of oxidative stress and inflammation in its development, phytomedicine is a good option for its control. Liver damage was induced in male C57BL/6J mice by chronic administration of angiotensin II (ANGII) (0.01 µg/kg/day, administered daily intraperitoneally). A hydroalcoholic extract of *Sechium edule* root (rSe-HA), standardized for its cinnamic acid content, was used to control the incidence of liver damage in mice (11 mg/kg/day of rSe-HA, administered orally). After 11 weeks, the mice were sacrificed and adipose tissue, serum, and liver were obtained. Hepatic cytokine and triglyceride (TG) concentrations were determined, and any histopathological changes were recorded. Meanwhile, ANGI treatment increased serum TG concentration (62.8%), alanine aminotransaminase (GPT/ALT) levels (206%), as well as TG accumulation (82.7%), hepatomegaly (32.1%), inflammation (measured by TNFα (70%), IL-1β (103%), IL-6 (92%), and TGFβ (203%) levels, along with inflammatory cell recruitment), and fibrosis with respect to untreated controls. rSe-HA prevented these increases, maintaining all parameters evaluated at values similar to those of the control group. Overall, our results support the hepatoprotective effects of rSe-HA against NAFLD and NASH, which are often the gateway to more severe pathologies.

KEYWORDS

inflammation, fibrosis, *Sechium edule*, hepatoprotective, angiotensin II, steatosis

1 Introduction

The early stages of some severe liver diseases are nonalcoholic fatty liver disease (NAFLD) and nonalcoholic steatohepatitis (NASH), which often progress to cirrhosis or liver carcinoma (Sheka et al., 2020). Since the only known treatment for these subsequent pathologies is liver transplantation (Sheka et al., 2020), there is a great need for treatment to control this process. NAFLD affects almost one-third of the world's population and is usually diagnosed in patients with comorbidities related to metabolic syndrome without excessive alcohol consumption, such as obesity and type 2 diabetes mellitus, hypertension without a history of hepatotoxicity, and viral infections (Younossi et al., 2016). Signs of a prooxidant and inflammatory environment observed in NAFLD, often leading to NASH (Rolo et al., 2012; Schuster et al., 2018).

The increased serum levels of angiotensin II (ANGII) that often accompany metabolic syndrome induce endothelial dysfunction (ED) (Savoia et al., 2011); both ED and ANGII itself are known to contribute to liver damage. Being the liver a highly vascularized organ (Schulze et al., 2019), the state of the endothelium is key to its good condition. Oxidative stress (OS) and inflammation are known to be central to the establishment and progression of liver damage (Wei et al., 2008), and both ED and ANGII induce a pro-steatotic environment, associated with elevated serum triglyceride levels and a pro-oxidant and pro-inflammatory condition (Wei et al., 2008; Sysoeva et al., 2017).

The current treatment of NASH, based on dietary and exercise interventions, has been shown to be effective, even in reversing fibrosis. Unfortunately, compliance with general measures involving lifestyle modifications is poor, making pharmacological strategies a necessary option (Oseini and Sanyal, 2017). To date, no single regular treatment is available for NASH; the signs of this disorder are consequences of a pro-steatotic environment, higher ANGII levels, systemic OS, and hypertriglyceridemia. Thus, the disease shows various therapeutic targets (Oseini and Sanyal, 2017; Rowe et al., 2022). Interestingly, phytomedicines, which usually include multiple active ingredients, could be specially well suited to help in this disease, so it is worth studying them.

Sechium edule (Jacq.) Sw. is a member of the Cucurbitaceae family native to Mexico (Cadena-Iñiguez, 2010). While there are no reports on its use in traditional medicine to treat liver diseases, other research groups have studied different parts of the plant for this purpose, with encouraging results (Firdous et al., 2012; Yang et al., 2015). However, the root had not been studied as a therapeutic tool in hepatic diseases. In a previous work by our research group, an acetone fraction of *S. edule* root (rSe-FA) was found to be effective in controlling ED induced in mice by

chronic administration of a sub-effective dose of ANGII; in that study, ANGII was found to induce morphological changes in the liver similar to those of NASH (Trejo-Moreno et al., 2021), and that administration of this fraction prevented such damage (Trejo-Moreno et al., 2018). Moreover, the fraction was rich in cinnamic and coumaric acids, whose antioxidant (Shen et al., 2019; Anlar, 2020) and anti-inflammatory properties (Karatas et al., 2020) have been widely reported. Thus, this work aims to study the hepatoprotective capacity of a hydroalcoholic extract of *S. edule* roots, standardized for its cinnamic acid content, in a murine model of liver damage induced by chronic administration of ANGII, which could resemble NASH (steatosis, hepatomegaly, hypertriglyceridemia, increased adipose tissue, necrosis, expression of proinflammatory interleukins, and fibrosis).

2 Materials and methods

2.1 Obtainment of hydroalcoholic extract

Roots of *Sechium edule* (Jacq.) Sw. (60 kg) were harvested in Cuautlapan, Veracruz, Mexico (18°47'00.5" N, 97°0'17.5" W, 1721 m above mean sea level) in February-March. All plant material was identified by Abigail Aguilar-Contreras (IMSS, Centro Medico Nacional, Mexico City). Voucher specimens were stored at this institution for future reference (IMSS-15549). Plant species were confirmed as *S. edule* and included in www.theplantlist.org (The plant List, 2013). Fresh roots were cut into small pieces with a stainless-steel knife and dehydrated in the dark under a continuous flow of air at 50°C for 72 h. The dried material (14.4 kg) was ground in a mill (Pulvex, Mexico City, Mexico) to 3–5 107 mm particles and extracted (8 kg) by maceration in an alcohol solution (12 L ethanol/H₂O 3:2 per 5 kg of plant material) for 24 h. The liquid extract was filtered and concentrated by vacuum distillation to obtain a semi-liquid extract, which was finally lyophilized to obtain 712 g of dry extract.

2.2 HPLC analysis

An HPLC analytical method was developed, using a Waters 2695 separation module (Waters Corporation, Milford, MA, United States). Secondary metabolites were detected with a Waters 996 photodiode array detector using Empower Pro software (Waters Corporation United States). Chromatographic separation was performed on a Supelcosil LC-F column (4 mm × 250 mm, 5 μm, Sigma-Aldrich, Bellefonte, PA, United States). The mobile phase consisted of

a gradient system of 0.5% trifluoroacetic acid aqueous solution (solvent A)—acetonitrile (solvent B), and the acetonitrile content was increased as follows: 0–1 min, 0% B; 2–3 min, 5% B; 4–20 min, 30% B; 21–23 min, 50% B; 24–25 min, 80% B; 26–27 min, 100% B; 28–30 min, 0% B. The flow rate was 0.9 ml/min, and the injection volume was 10 μ L. The detection wavelength was 280 nm. Cinnamic acid was identified by comparing retention times (RT) and UV spectra with a commercial standard (Sigma-Aldrich). The RT of cinnamic acid was 12.4 min ($\lambda = 219, 280$ nm).

2.3 Quantification of cinnamic acid in rSe-HA

A calibration curve for cinnamic acid was plotted using a commercial standard of the substance. Six concentrations of cinnamic acid (3.12, 6.25, 12.5, 25, 50, and 100 μ g/ml) were analyzed in triplicate as described above, yielding a linear plot with a good coefficient of determination ($y = 1945.6x - 461.88$, $r^2 = 0.999$). An analysis of the signal-to-noise ratio indicated a limit of quantification (LOQ) ≥ 0.3 μ g/ml. The amount of cinnamic acid in the hydroalcoholic extract was calculated by the area under the corresponding peak on the standard curve. The mean results are expressed as mg cinnamic acid/g dry extract. This value was used to determine the dose of extract to be administered to the mice.

2.4 Animals and experimental groups

Male C57BL/6J mice (19–21 g) from our animal facility were used. The animals were distributed in groups of eight mice each, housed and maintained in pathogen-free conditions in the animal house of the Faculty of Medicine of the Autonomous University of Morelos (FM-UAEM) under constant temperature (21–23°C) and humidity (45–50%) and a 12-h light/dark cycle. All experiments were performed in accordance with the National Institutes of Health Guide for the Care and Use of Laboratory Animals and were reviewed and approved by the Ethical Committee for the Care and Use of Laboratory Animals (Permit No. 005/2011) of the FM-UAEM.

One Vehicle group was administered water only. The remaining three groups were treated with ANGII (Sigma, St. Louis, MO, United States) i. p., 0.01 μ g/kg/day (ANGII) (Trejo-Moreno et al., 2021), for 11 weeks, either alone or co-administered p. o. with Losartan (LOS) (Cozaar[®], Merck Sharp & Dohme, Kenilworth, NJ, United States) at a dose of 10 mg/kg diluted in 0.2% carboxymethylcellulose (CMC, Maquimex, Mexico) (Bastaki, et al., 2018) or rSe-HA diluted in water, at a dose of 11 mg/kg, for 11 weeks. Both treatment time and the dose administered were based on data previously reported by Trejo-Moreno et al. (2018). Dose calculation was

based on the concentration of cinnamic acid in the HA extract, which in turn was calculated based on the concentration of the same molecule in the acetone extract used by Trejo-Moreno et al. (2018).

2.5 Serum, liver, and adipose tissue collection

After treatment (at week 11), mice were anesthetized with sodium pentobarbital (i.p., 30 mg/kg) and bled through the retro-orbital venous sinus. To collect serum, heparinized blood was centrifuged at 534 $\times g$ for 8 min at room temperature, and the serum was frozen at -80°C until use. Mice were then perfused with ice-cold phosphate buffered solution (PBS) (140 mM NaCl, 2 mM KCl, and 1.15 mM K_2HPO_4) (Sigma, St. Louis, MO, United States). Whole liver, as well as epididymal, mesenteric, subcutaneous and perirenal adipose tissues were retrieved, weighed, and frozen at -80°C until use. For histopathological studies, mice were perfused with PBS and then buffered formalin (PBS + 10% formaldehyde, pH 7.0). The organs were then collected and fixed in the same solution.

2.6 Quantification of serum alanine transaminase

Liver enzymes were measured in mouse serum according to the International Federation of Clinical Chemistry (IFCC) method, using a commercial GPT/ALT kit (QCA, Amposta, Tarragona, Spain), according to manufacture instruction.

2.7 Quantification of serum triglycerides

Triglycerides (TG) were quantified in mouse serum samples by a colorimetric method using the Triglycerides-LQ kit (QCA), following the manufacturer's instructions.

2.8 Liver homogenates to quantify cytokines and TGs

Cytokines and TGs were quantified in mouse liver homogenate supernatants. For TG determination, liver samples were suspended 1:10 w/v in lysis buffer (NaCl 140 mM; Tris-HCl 50 mM; 0.01% Triton x-100) in a D-160 rotary homogenizer (DLab Scientific, Beijing, China). The suspension was centrifuged at 580 $\times g$ for 8 min at 4°C, and the supernatant was stored at -80°C . For cytokine determination, liver samples were suspended 1:10 w/v in cold 0.1% PBS-PMSF (phenylmethylsulphonyl fluoride) (Sigma, St. Louis, MO,

United States). Homogenates were centrifuged at $1879 \times g$ for 8 min at 4°C, and supernatants were stored at -80°C.

2.9 Cytokine quantification by ELISA

Several ELISA kits were used to determine cytokine concentration, following the manufacturer's instructions. OptEIA ELISA kits for interleukin 1 β (IL-1 β), IL6, tumor necrosis factor α (TNF α), and mouse transforming growth factor β (TGF β) were purchased from BD Biosciences (Franklin Lakes, NJ, United States). Briefly, 96-well, flat-bottom ELISA plates (Nunc ImmunoPlate) were coated with the respective capture antibody and incubated overnight at 4°C in carbonate buffer (pH 9.6). Non-specific binding sites were blocked by incubating for 30 min at room temperature (RTemp) with PBS-5% fetal bovine serum. Liver extracts were added and incubated for 2 h at RTemp. The plates were then incubated with the corresponding horseradish peroxidase (HRP)-conjugated anti-cytokine detection antibody for 30 min at room temperature. Bound complexes were detected by reaction with tetramethylbenzidine (TMB) (Invitrogen, Carlsbad, CA, United States) after 30 min incubation in the dark. The reaction was stopped with 2N H₂SO₄ and OD was measured at 450 nm at 37°C on a VERSAmax ELISA plate reader (Molecular Devices). Standard curves were prepared to calculate the concentration of each cytokine. Concentrations were expressed as pg/mg protein.

2.10 Quantification of hepatic triglycerides

Liver TG was analyzed as described in Section 2.7, in samples obtained as described in Section 2.8.

2.11 Histopathology

Mouse livers were prepared for sectioning in paraffin. Sections (5 μ m) were transferred to poly-L-lysine-coated slides (Sigma, St. Louis, MO), deparaffinized and rehydrated. For histopathological studies, sections were stained with Masson's trichrome technique (MT). This method combines hematoxylin staining with cytoplasmic and connective tissue staining (Goldner, 1938; Bastaki et al., 2018). All slides were observed under an ECLIPSE 80i microscope (Nikon Instruments, Tokyo, Japan), and images were processed with Metamorph v.6.1 software (Molecular Devices). The number of Mallory bodies and collagen fiber accumulations on Masson-stained slides were counted. To count Mallory bodies, 50 fields per section were analyzed at 40X magnification in three sections per mouse and three mice per condition. The presence of collagen was analyzed with Metamorph software in 50 fields

per section under 40X magnification in three sections per mouse and three mice per condition.

2.12 Statistical analysis

All measured parameters were compiled in Excel (Microsoft Co., Redmond WA, United States). Data are presented as box-and-whisker plots. Groups or treatments were compared by one-way ANOVA with a Tukey-Kramer post-hoc test. Data were analyzed with GraphPad InStat v.3.06 software (GraphPad, San Diego, CA, United States). Differences were considered as significant for $p \leq 0.05$.

3 Results

3.1 A dose of 11 mg/kg/day was determined for rSe-HA

To administer a dose of rSe-HA equivalent to the dose of rSe-FA administered in a previous study (Trejo-Moreno et al., 2018), both extracts were standardized to determine their content of the most abundant compound, cinnamic acid. rSe-HA and rSe-FA were characterized chromatographically by HPLC, as shown in Figure 1A. The RT for the standard cinnamic acid was 12.10 min, and this substance was detected in both rSe-HA and rSe-FA, with an RT of 12.13 and 12.15 min, respectively (Figure 1). This result was verified by comparing a UV spectrum of standard cinnamic acid and rSe-HA; both spectra showed an absorbance maximum at 216.9 and 276.9 nm. Based on the RT values and UV spectra, coumaric acid was also identified in rSe-HA, as shown in Table 1. Two other unknown molecules were found, with retention times of 6.995 and 9.075 min. A standard concentration vs. absorbance curve for cinnamic acid was linear ($y = 1945.6x + 461.88$) over the concentration range of interest. Using this curve, a cinnamic acid concentration of $161 \pm 0.00 \mu\text{g/g}$ and $141.76 \pm 0.00 \mu\text{g/g}$ was calculated at rSe-FA and rSe-HA, respectively. Based on these results, mice were administered a total dose of 11 mg/kg/day of rSe-HA, equivalent to the concentration used in a previous work with rSe-FA (Trejo-Moreno et al., 2018).

3.2 rSe-HA prevents triglyceride accumulation

Triglyceride accumulation in hepatocytes is often the first sign in various liver diseases (Kawano and Cohen, 2013). To determine whether rSe-HA controls this process, TGs were quantified in mouse liver samples, along with the degree of hepatomegaly and the occurrence of histopathological changes in the organ.

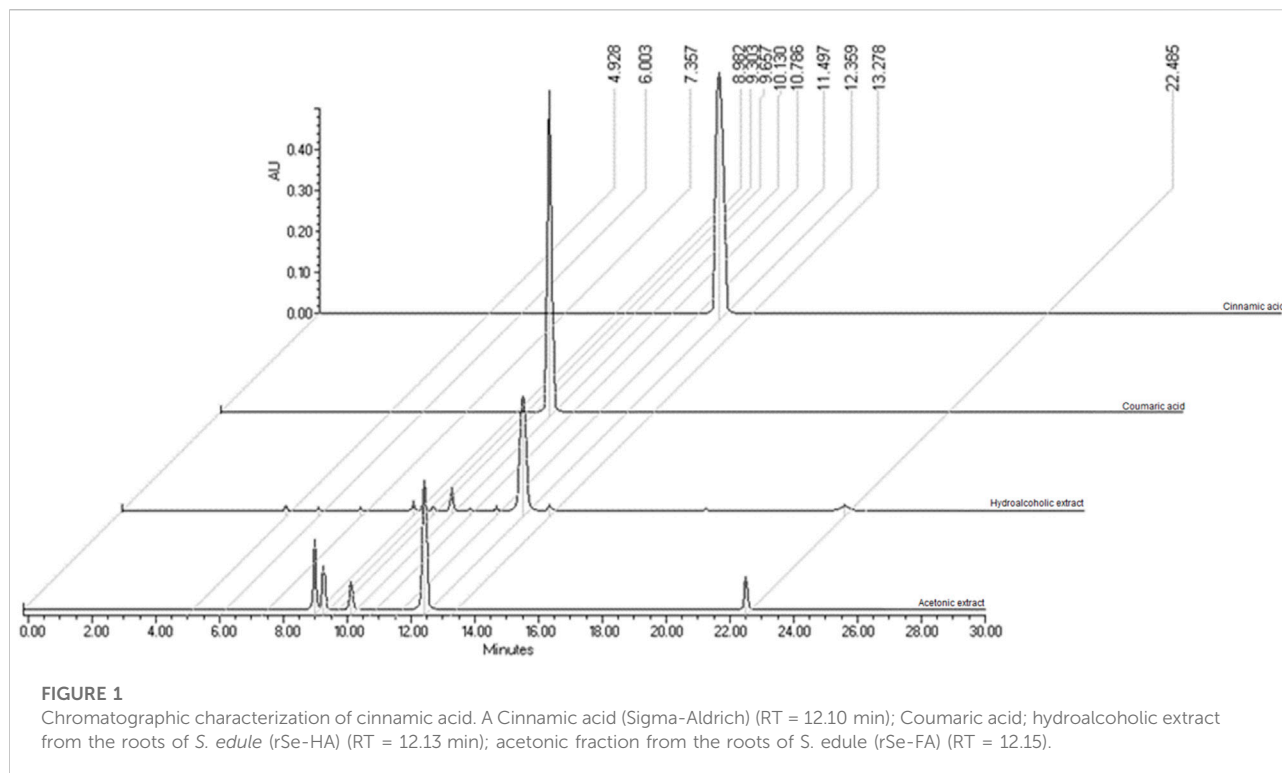
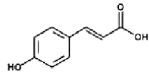
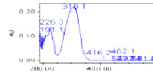
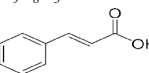
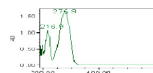


TABLE 1 Molecules identified in the extracts based on retention times. $\lambda = 216.9, 276.9$ nm.

RT (min)	P No	PC	MW	Theoretical m/z	Positive mode measured m/z	Error	Fragments	Structure and molecular formula	UV	Bioactivity reported
9.98	3	Coumaric acid	164.04	164.93	165.06	0.06	141.01; 82.90	 <chem>O=C(O)/C=C/c1ccc(O)cc1</chem>		Antioxidant Shen et al. (2019)
12.13	4	Cinnamic acid	148.15	148.96	149.06	0.04	130.93; 82.93	 <chem>O=C(O)/C=C/c1ccccc1</chem>		Antioxidant and anti-inflammatory Anlar, (2020); Karatas et al. (2020)

RT, retention time; P. No, Peak Number; PC, proposed compound; MW, molecular weight; UV, ultraviolet spectrum.

As shown in Figure 2A, i. p. administration of ANGII led to lipid accumulation in the liver, increasing TG levels by 82.7% with respect to the vehicle-administered group and the rSe-HA-treated group ($p < 0.001$). On the other hand, no significant differences were observed between mice treated with ANGII + rSe-HA and the vehicle-administered group; however, an increase of 167% in hepatic TG levels was observed in mice co-treated with losartan ($p < 0.001$) with respect to vehicle-administered animals. With regard to hepatomegaly (as measured by liver weight), no differences were observed between ANGII + rSe-HA-treated mice and

vehicle-administered animals, whereas significant increases of 32.1% and 39.1% in liver weight was observed in ANGII and ANGII + losartan-treated mice compared with vehicle-treated animals ($p < 0.05$) (Figure 2A). Histopathological studies indicated that hepatocytes in the ANGII-treated group showed a severe diffuse pattern (arrow), particularly in the subcapsular areas and in the liver parenchyma near the portal triads (Figure 2D,H), but not in the central vein area (Supplementary Figure S1). Within the hepatocytes, the nucleus is displaced, which could be due to lipids clustered in microvesicles. A similar pattern was observed in the ANGII

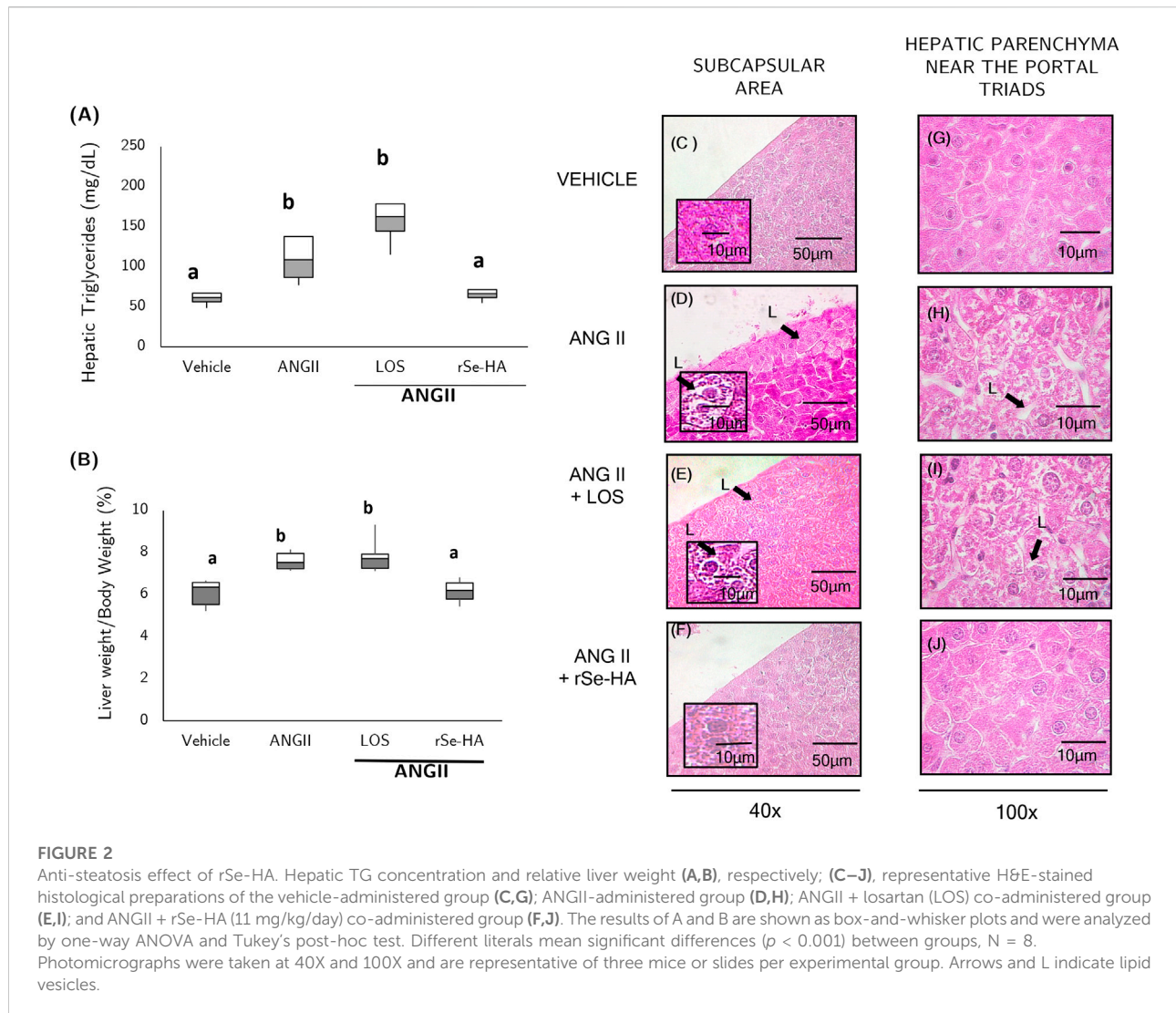


FIGURE 2

Anti-steatosis effect of rSe-HA. Hepatic TG concentration and relative liver weight (A,B), respectively; (C–J), representative H&E-stained histological preparations of the vehicle-administered group (C,G); ANGII-administered group (D,H); ANGII + losartan (LOS) co-administered group (E,I); and ANGII + rSe-HA (11 mg/kg/day) co-administered group (F,J). The results of A and B are shown as box-and-whisker plots and were analyzed by one-way ANOVA and Tukey's post-hoc test. Different literals mean significant differences ($p < 0.001$) between groups, $N = 8$. Photomicrographs were taken at 40X and 100X and are representative of three mice or slides per experimental group. Arrows and L indicate lipid vesicles.

+ losartan treated group (Figure 2E,I). Interestingly, none of the ANGII-induced changes were observed in the group coadministered with ANG II + rSe-HA (Figure 2F,J), which showed similar results to those observed in vehicle-treated mice (Figure 2C,G), correlating with hepatic TG levels (Figure 2A) and relative liver weight (Figure 2B). These results indicate that rSe-HA was effective in preventing lipid accumulation resulting from chronic ANGII administration.

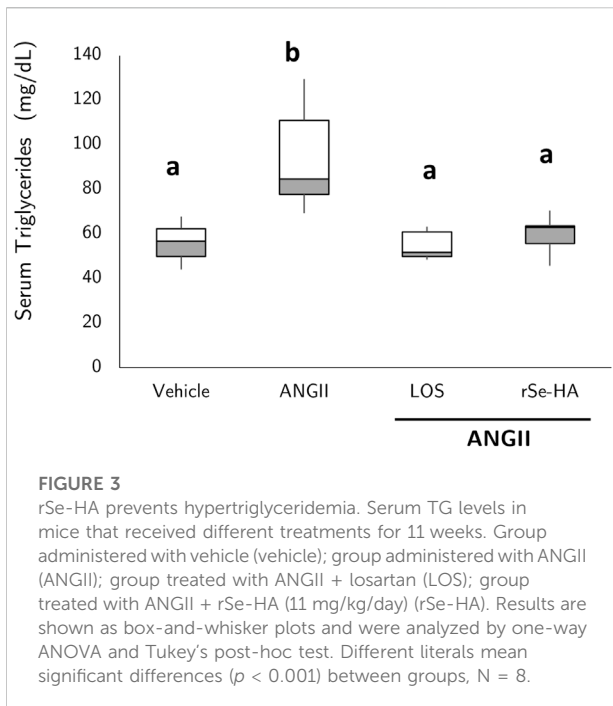
3.3 rSe-HA prevents ANGII-induced hypertriglyceridemia

Clinically, hepatic lipid accumulation is accompanied by an increase in blood TG levels, in the context of dyslipidemia that characterizes NASH and NAFLD (Koo, 2013). To determine the

effect of rSe-HA on hypertriglyceridemia, TG levels were assessed in serum samples from mice given the different treatments. As shown in Figure 3, ANGII administration led to an increase of 62.8% in serum TG levels (hypertriglyceridemia) with respect to mice administered with vehicle ($p < 0.001$), whereas no significant increases were observed in animals administered with ANGII + losartan nor in those administered with ANGII + rSe-HA. This result indicates that rSe-HA prevented hypertriglyceridemia despite the chronic presence of ANGII.

3.4 rSe-HA prevents body-weight gain resulting from increased adipose tissue

An increase in adipose tissue has been observed in conditions involving liver damage, such as NASH (Kawano and Cohen, 2013), related to hypertriglyceridemia and lipid

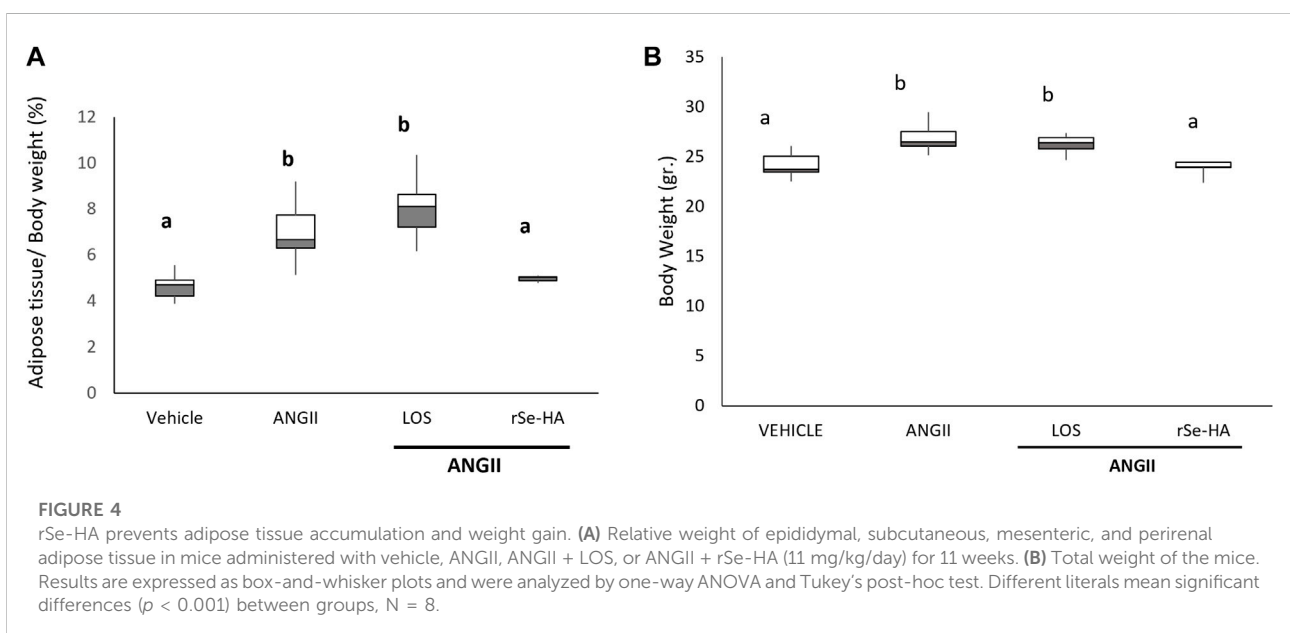


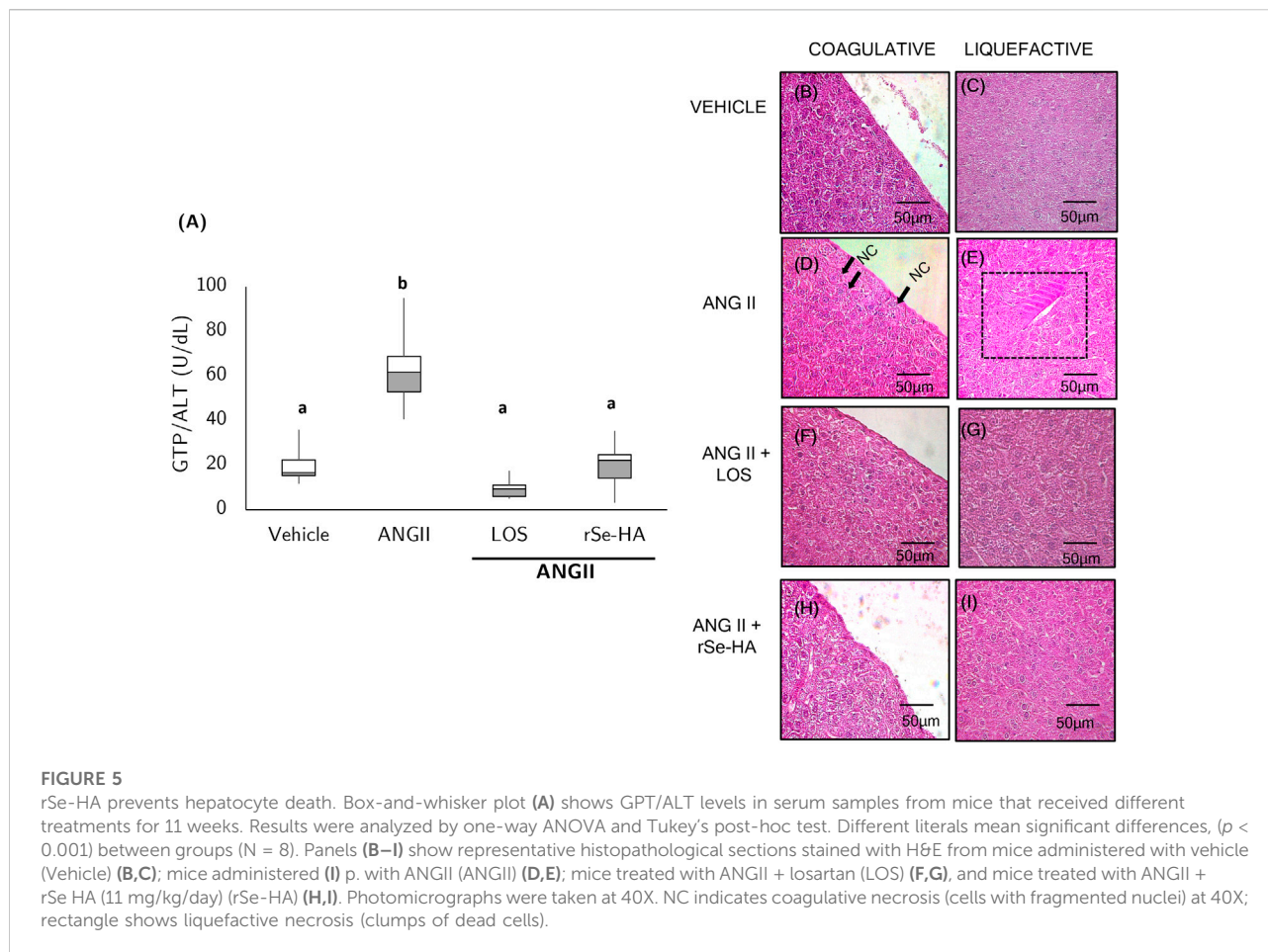
accumulation in the liver (Polyzos et al., 2017); this can be linked to an increase in body weight as well (Kawano and Cohen, 2013). As shown in Figure 4A, the relative weight of adipose tissue (mesenteric, epididymal, perirenal, and subcutaneous) increased by 48.9% in ANGII-treated mice relative to animals receiving vehicle ($p < 0.05$). The group co-administered with ANGII + losartan also showed an increase in adipose tissue mass (173%, 73.8%, and $p < 0.05$)

relative to the vehicle-administered group, but it was not significantly higher than in the group treated with ANGII alone. In contrast, no significant change was observed in animals receiving ANGII + rSe-HA relative to the vehicle-treated group. These results correlated directly with the total weight of the animals, since those treated with ANGII showed an increase of 6% in weight ($p < 0.05$); this trend was the same in the group treated with losartan, but it was prevented by the extract (Figure 4B). This indicates that rSe-HA prevents ANGII-induced adipose tissue accumulation, and the ensuing weight gain in the animals. The effect of each treatment on each adipose tissue is presented in Supplementary Figure S2.

3.5 rSe-HA prevents increased serum GPT/ALT levels and liver damage

Increased levels of alanine aminotransferase (GPT/ALT) could indicate cell death by necrosis (Alarcón Corredor et al., 1998). Serum GPT/ALT levels were evaluated in mice to determine the protective effect of rSe-HA against ANGII-induced liver damage. As shown in Figure 5A, GPT/ALT levels were significantly higher in ANGII-treated mice (206%, $p < 0.001$) relative to vehicle-administered animals, as well as with respect to rSe-HA- and losartan-treated mice. This finding is consistent with histopathological evidence, as moderate and diffuse coagulative (Figure 5D) and liquefactive (Figure 5E) necrosis patterns were observed near the portal triad and in subcapsular areas in liver sections of ANGII-treated mice. These patterns of cell death were not observed in the vehicle-administered group (Figures 5B,C), in the ANGII + losartan-treated group (Figures 5F,G), or in the ANGII + rSe-HA-treated





group (Figures 5H,I). This indicates that rSe-HA prevents hepatocyte cell death by necrosis induced by chronic ANGII administration.

3.6 rSe-HA prevents inflammation

Inflammation is a major contributor to NASH progression. In mice, necrosis and the overall metabolic state produce damage-associated molecular patterns (DAMPs), which are strong inducers of inflammation (Schuster et al., 2018). This proinflammatory state is evidenced by the expression of cytokines and by the presence of immunoinflammatory cellular infiltration, mainly neutrophils and lymphocytes (Wei et al., 2008; Schuster et al., 2018). To determine the effect of rSe-HA on liver inflammation, cytokines such as IL1 β , IL6, and TNF α were quantified by sandwich ELISA. In addition, histopathological studies of the liver were performed to detect the presence of inflammatory cell foci. As shown in Figures 6A–C, chronic administration of ANGII led to a significant increase in the levels of the proinflammatory cytokines TNF α

(70%), IL-1 β (103%), IL-6 (92%), relative to the vehicle-administered group ($p < 0.0001$). On the other hand, no significant differences were found in the expression of the three cytokines between mice co-administered with ANGII + rSe-HA and those administered with vehicle. This result agrees with the histopathological findings in liver tissues (Figures 6H,J). Lymphocytes and macrophages were found in several areas of the liver of ANGII-treated mice; they were very abundant and showed a severe diffuse pattern in the peri-hepatic fat (Figure 6H), with a moderate focal pattern in the liver parenchyma, forming foci of inflammatory cells in the vicinity of the peri-portal areas (Figure 6I) that were significantly increased (Figure 6D) and showed a severe diffuse pattern in the subcapsular areas (Figure 6J). In contrast, no foci of cellular infiltration were found in liver samples from mice co-administered with either ANGII + losartan (Figures 6K–M) or ANGII + rSe-HA (Figures 6N–P). These results indicate that rSe-HA is effective in controlling cell infiltration and, together with the control in proinflammatory cytokine expression in liver cells induced by ANGII, they highlight its anti-inflammatory effect.

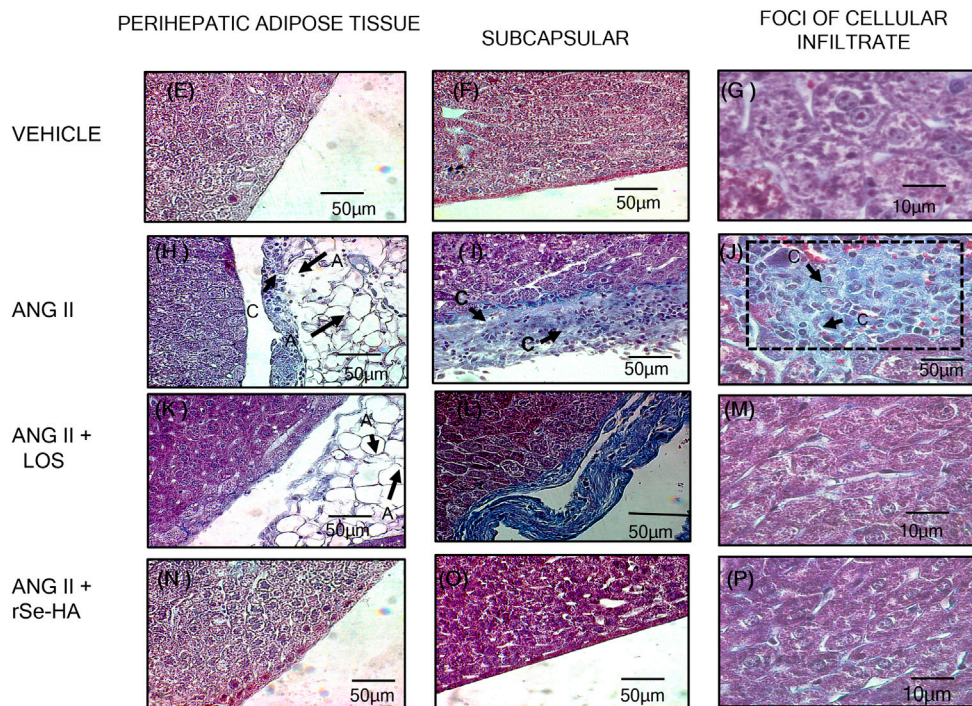
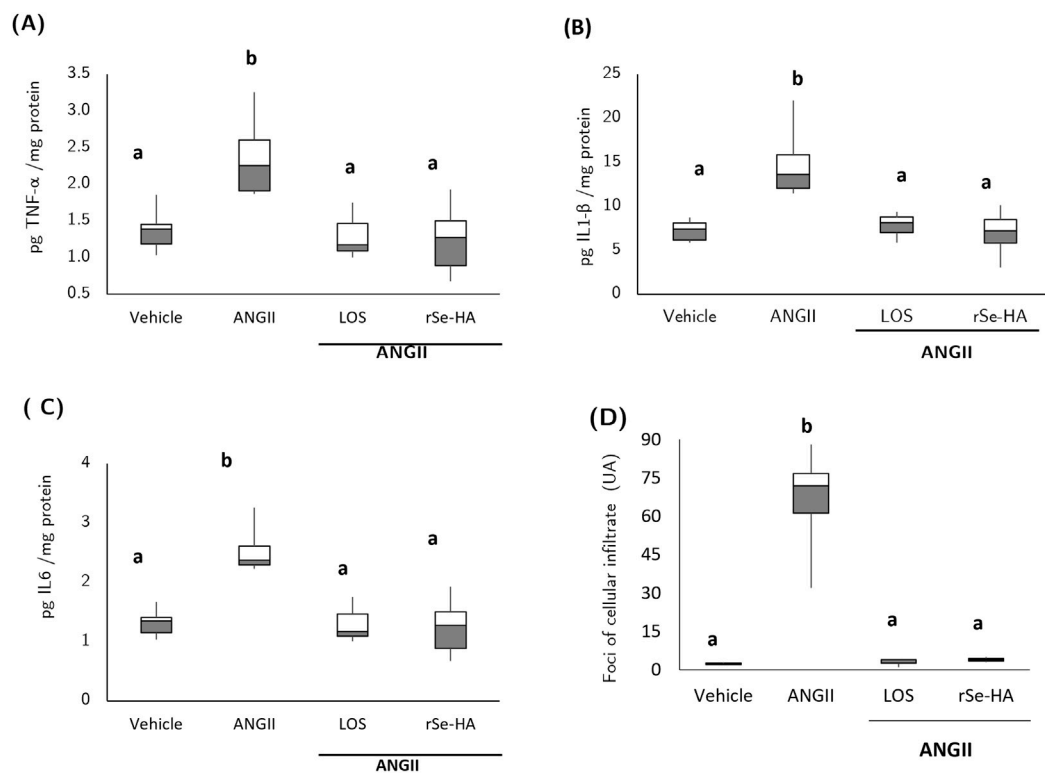
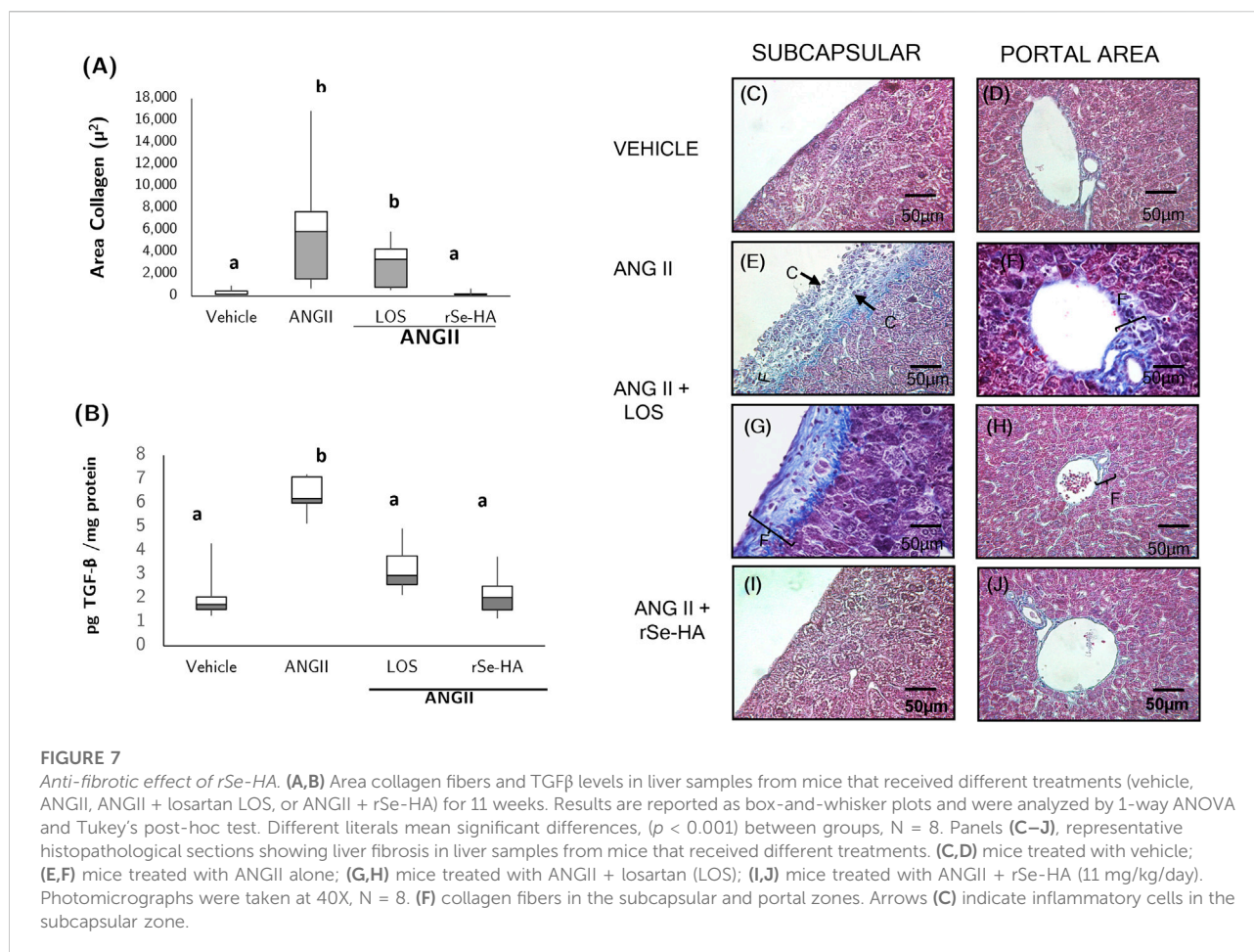


FIGURE 6

Anti-inflammatory effect of rSe-HA. Box-and-whisker plots (A–C) show the levels of TNF α , IL1 β , and IL6; (D) inflammatory cell foci were counted in liver tissue samples from mice receiving different treatments (vehicle, ANGII, ANGII + LOS or ANGII + rSe-HA) for 11 weeks. Results are presented as box-and-whisker plots and were analyzed by one-way ANOVA and Tukey’s post-hoc test. Different literals mean significant differences, ($p < 0.001$) between groups ($N = 8$); panels (E–P) show representative liver histological sections stained with Masson’s trichrome method in three mice per group. photomicrographs were taken at 40X (E,F,H,I,K,L,N,O) and 100X (G,J,M,P). A = adipocytes; C and rectangle = inflammatory cells.



3.7 rSe-HA prevents hepatic fibrosis

Hepatic fibrosis, defined as an excessive accumulation of collagen in the extracellular matrix (ECM) of the liver, is a hallmark of chronic liver conditions such as NASH; TGF β is a major inducer of this response, activating stellate cells and transforming them into myofibroblasts (Bataller and Brenner, 2005). To evaluate the protective effect of rSe-HA against liver fibrosis, histological liver sections from mice that received the different treatments were stained with Masson's trichrome method and observed under the microscope (Figure 7), and this was related to the levels of TGF β in the liver.

Both histopathological analysis and measurement of the tissue area covered by collagen fibers indicate that treatment with rSe-HA prevented collagen accumulation (Figures 7A,E,F) induced by ANGII treatment. This hormone significantly increased collagen accumulation (Figure 7A), which was observed as a blue-stained area indicating subcapsular fibrosis (Figure 7E), together with a moderate diffuse pattern in the portal triad (Figure 7F). Accumulation of collagen fibers was also observed in the losartan-treated group (Figure 7A). These results are in agreement with TGF levels in the liver. No

significant differences in TGF levels were observed between animals administered with rSe-HA and the vehicle-treated group, despite the presence of ANGII. On the other hand, TGF levels were significantly higher in the ANGII-only treated group (203%, Figure 7B). This result indicates that rSe-HA prevents liver fibrosis typically associated with NASH.

4 Discussion

In this work, we demonstrated the efficacy of the hydroalcoholic extract of *S. edule* roots in controlling the pathological conditions that often accompany NASH, such as hepatomegaly, hypertriglyceridemia, and adipose tissue enlargement, effectively controlling triglyceride accumulation in the liver, necrosis, inflammation, and fibrosis. This study confirms the previously reported association between the chronic administration of ANGII by the i. p. route and the development of metabolic alterations in the liver (Trejo-Moreno et al., 2018, Trejo-Moreno et al., 2021).

In previous studies, we reported that administration of 10 mg/kg of the acetone fraction of rSe-HA counteracted histopathological liver

damage resembling NASH induced by chronic ANGII i. p. application. However, plant extract fractions obtained with acetone are not an optimum choice for human consumption (Farmacovigilancia, 2015; de insumos de la salud, 2021); therefore, the rSe-HA from which the acetone fraction was obtained was evaluated herein (Trejo-Moreno et al., 2018). Coumaric acid, the second most abundant molecule in rSe-HA (Figure 1A), could provide the extract with antioxidant properties along with cinnamic acid (Shen et al., 2019; Anlar, 2020); the latter compound has also been shown to exert anti-inflammatory effects (Karatas et al., 2020). Both major components of rSe-HA could explain the efficacy of the extract in controlling NASH-like liver damage, as ANGII is known to induce oxidative stress and an inflammatory state (Wei et al., 2008; Trejo-Moreno et al., 2021). It should be noted that the dose used in this work is lower than those administered in studies conducted with aerial parts of the plant; previous studies used leaf or stem extracts at 0.1–0.5%, which is approximately equivalent to 1–5 g/kg (Yang et al., 2015) or 100–200 mg/kg of fruit extracts (Firdous et al., 2012); this could suggest a greater potency in root-derived extracts.

ANGII is a pleiotropic hormone. Although its effects are different depending on the target cell (Patel et al., 2017), it generally induces oxidative stress and inflammation (Wei et al., 2008; Trejo-Moreno et al., 2021) and plays a role in the development of metabolic diseases such as NASH (Wei et al., 2008; Rolo et al., 2012). Our results indicate that ANGII induced, on one hand, adipocyte hyperplasia and hypertrophy and the weight of the tissue and directly impacting on total weight gain in mice (Figures 4A,B); on the other hand, it also induced hepatic steatosis and hepatomegaly (Figures 2A,B,D,H). Steatosis was observed in the subcapsular zone and in the parenchyma near the portal triads, as reported by other authors for nonalcoholic steatosis (Rappaport, 1958, Rappaport, 1973; Koo, 2013), in contrast to the pattern described for alcoholic steatosis, in which lipid accumulation occurs in areas adjacent to the central vein (Rappaport, 1958, Rappaport, 1973).

Administering the hydroalcoholic extract prevented this accumulation, whereas losartan did not. This is interesting, because the effect of ANGII on adipocytes does not seem to occur only through AT1R (which is antagonized by losartan) but also through ATR2 (Patel et al., 2017; Sysoeva et al., 2017). Meanwhile, in hepatocytes, which do not express ATR2 (Paizis et al., 2002; Wei et al., 2008), this effect has been suggested to be due to the activation of the sterol regulatory element-binding protein 2 (SREBP2) by ANGII, which induces the *de novo* synthesis of oleic acid, using glucose as a raw material (Yang et al., 1997; Strable and Ntambi, 2010). Oleic acid and other free fatty acids thus produced are esterified in the cell to TGs by enzymes synthesized after SREBP2 activation. In addition, it has been reported that ROS (Sekiya et al., 2008) produced in the pro-oxidant and pro-inflammatory state induced by ANGII (Wei et al., 2008; Trejo-Moreno et al., 2021) activate PPAR γ , (Marion-Letellier et al., 2016), thus enhancing steatosis. On the other hand,

losartan prevented the increase in serum TG levels, as since adipose tissue depends on ATR2 for its activity, thus favoring the increase of functional adipose tissue and total weight (Figure 4) while preventing the release of TGs and free fatty acids into the serum (Figure 3). Interestingly, although hepatocytes do not express ATR2 and losartan antagonizes ATR1, steatosis was not prevented, indicating that another pathway is being activated. Losartan has been reported to activate the transcription factor PPAR γ and promote TG synthesis in adipose tissue (Schupp et al., 2004), which could also occur in hepatocytes, as it was observed to stimulate TG synthesis in the liver.

The observed effect of rSe-HA against adipose tissue hyperplasia and hepatic steatosis is consistent with that reported by Yang et al. (2015), who demonstrated that the administration of methanolic extract of *S. edule* leaves, rich in coumaric acid among other polyphenols, controlled adipose tissue hyperplasia and hypertrophy, as well as hepatic steatosis in obese rats, indicating the effectiveness of these molecules in preventing hepatic damage (Yang et al., 2015). In addition, rSe-HA controlled hypertriglyceridemia (Figure 3), which is caused by adipose tissue dysfunction and plays a major role in the development of steatosis (Koo, 2013; Polyzos et al., 2017). This result is in agreement with the effect observed in 2021 by Sudargo et al. who reported that *S. edule* fruit extract in obese rats decreased the concentration of blood lipids, including free fatty acids, triglycerides, and low- and very low-density lipoproteins (Sudargo et al., 2021). Several authors suggest that cinnamic and coumaric acids activate kinases that increase catabolism, such as AMPK (Yoon et al., 2013; Kopp et al., 2014; Nguyen et al., 2021; Wu et al., 2021), and inactivate transcription factors involved in lipogenesis such as SREBP2 and PPAR γ (Kishida et al., 2014, Kishida et al., 2015; Aranaz et al., 2019) thus, the possible mechanism underlying its efficiency could be related to both actions, independently of the actions of all the other molecules in the extract.

As shown in Figure 5, rSe-HA prevented necrosis. In this work, necrosis was evidenced by serum GPT/ALT levels and histopathological findings. By the type of necrosis identified in histopathological studies, the damage can be classified into two phases: in the coagulative phase, nuclei are diffuse, and the structure of dead tissue is maintained, until finally the cells are eliminated by phagocytosis, becoming liquefactive necrosis, whereby the tissue is transformed into a viscous and liquid mass at focal points (Uri-Flores 2021). Both necrosis types were found in two areas: 1) the periportal zone (near the portal triad) and 2) the subcapsular zone (in the periphery of the liver) (Figure 2D) in ANGII-treated mice. Precisely, it has been reported that hepatocytes in portal and subcapsular zones actively participate in fatty acid β -oxidation in NASH (Rappaport, 1958, 1973), which could be related to a strong oxidative stress that, as mentioned above, induces necrosis and inflammation (Rolo et al., 2012). This effect was very efficiently counteracted by rSe-HA, and it can be inferred that the cinnamic and coumaric acids in the extract acted through two distinct pathways: 1) by scavenging free radicals (Shen et al., 2019; Anlar, 2020) and 2) by activating nuclear factor erythroid-derived factor

2 (Nrf2) (Nguyen et al., 2009; Sabitha et al., 2020), which promotes the synthesis of antioxidant enzymes such as homoxygenase-1, glutathione-S-transferase A1, and NAD(P)H-quinone oxidoreductase (Nguyen et al., 2009; Sabitha et al., 2020), thus preventing oxidative damage produced by ANGII. Indeed, the effect of cinnamic and coumaric acids on necrosis had been previously reported in other models. In these studies, the activity of serum ALT was reduced by cinnamic and coumaric acids in rat models of hepatic necrosis induced by exposure to D-Galactosamine and gamma radiation or by the oral administration of carbon tetrachloride, respectively (Ibrahim et al., 2020; Aldaba-Muruato, et al., 2021). Considering that the extract was as effective as losartan, it can be inferred that AT1R has a major influence on the generation of necrosis.

Inflammation plays a major role in the progression of chronic liver diseases such as NASH, and both the extract and losartan efficiently controlled the expression of IL1 β , TNF α , and IL6 (Figure 6A–C), as well as the presence of inflammatory cells (Figures 6D, H–J) both diffusely and in inflammatory foci. These results are consistent with those published by other authors, who indicated that ANGII activates macrophages through AT1R (Doyon and Servant, 2010; Yamamoto et al., 2011); moreover, ROS themselves are recognized as damage-associated molecular patterns, which potentiate the proinflammatory state (Frantz et al., 2001; Birch et al., 2021). On the other hand, the efficacy of the extract to counteract inflammation may be due to the inhibition of NF κ B expression by both cinnamic and coumaric acid, preventing the phosphorylation of I κ B (Neog et al., 2017; Sabitha et al., 2019) induced by the steatotic and prooxidant state in the cell (Wei et al., 2008; Schuster et al., 2018), preventing the activation of NF κ B and its translocation to the cell nucleus. Finally, among the interleukins evaluated is TGF β , which has been reported to induce fibrosis (Gressner et al., 2002). This, like the other interleukins evaluated, was found in similar concentrations in the animals that received rSe-HA and the controls that were given vehicle. This result is compatible with the absence of collagen fibers observed according to Masson's technique in the liver of mice co-treated with rSe-HA and ANGII (Figures 7I,J), in contrast to animals that only received ANGII, where they were significantly increased (Figures 7D,E). In the liver of these mice, the fibers were found in the subcapsular and portal areas, the same areas where necrosis was observed, reported as the onset of a cirrhotic process (Wei et al., 2008). In addition, ANGII interacts with ATR1 and TGF β 1 receptors of stellate cells, activating them and transforming them into myofibroblasts, thus participating in the synthesis of collagen fibers (Gressner et al., 2002; Lugo-Baruqui et al., 2010) and contributing to fibrosis. Both cinnamic acid and coumaric acid have been reported to inhibit fibrosis by activating the nuclear factor Nrf2 (Hseu et al., 2018; Sabitha et al., 2020), which not only protects cells from oxidative damage (Nguyen et al., 2009) but also prevents liver injury and helps repair fibrosis by inducing the production of enzymes that degrade excess extracellular matrix and prevent collagen synthesis (Aleksunes and Manautou, 2007).

While our discussion focused on the effects reported for cinnamic acid and coumaric acid, the most abundant molecules in the extract, we should bear in mind that an advantage of phytomedicines is that they are composed of multiple molecules with different therapeutic targets. Since liver diseases such as NASH are multifactorial, a phytomedicine such as rSe-HA is a good choice to prevent their progression. It has been reported that *S. edule* is rich in polyphenols and terpenes (Costet Mejia, 2020); on the one hand, these compounds inactivate lipid anabolism, and on the other hand, they activate lipid catabolism (Kopp et al., 2014; Kishida et al., 2015; Nguyen et al., 2021). In addition to their antioxidant and anti-inflammatory effects (Shen et al., 2019; Anlar, 2020; Karatas et al., 2020), this explains the effectiveness of the extract. Herein, we have demonstrated that rSe-HA controlled efficiently the NASH-like liver damage induced by a chronic application of ANGII. This could be explained by the fact that the effects of ANGII are based on the induction of a prooxidant and proinflammatory state, which is counteracted by cinnamic and coumaric acids, along with other polyphenols and terpenes contained in the extract. This is an encouraging result, because to date there is no pharmacological treatment to control this type of liver disease, of which fat accumulation in hepatocytes is the starting point.

Data availability statement

The original contributions presented in the study are included in the article/Supplementary Material, further inquiries can be directed to the corresponding author.

Ethics statement

The animal study was reviewed and approved by Ethical Committee for the Care and Use of Laboratory Animals (Permit No. 005/2011) of the FM-UAEM.

Author contributions

Conceptualization: ZA-AO and G-RS; fund acquisition: GF and G-RS; investigation: ZA-AO, and G-RS; methodology: ZA-AO, A-CM, AZ, J-CT, JC-BR, C-TM, M-MM, and G-CM; resources: GF; supervision: ZA-AO, G-AR, and G-RS; writing—original draft: ZA-AO, G-RS, and AZ; writing—review & editing: ZA-AO, EJ-JF, AZ, GF, and G-RS.

Acknowledgments

The authors thank Juan Francisco Rodriguez for copyediting the original manuscript; thanks to Lic. Nohemi Gelista Herrera and M.C. Vanesa Báez Gelista for their support in histological techniques;

thanks to Biol. Ana Luisa Ocampo Ruiz, Biol. Julieta Hernández Acosta, Biol. Patricia Solís Rosales and M.C Juan Carlos Villegas García, Dra. María Dolores Pérez García for their technical support; thanks to M.C. Nancy Arias García for her technical support in the vivarium. MM and CT-M thank to CONACYT for the post-doctoral fellowship (I1200-94-2020 and I1200/320/2022, respectively). Zimri Aziel Alvarado-Ojeda thanks CONACYT for the postgrad fellowship (1019271).

Conflict of interest

The authors declare that the research was conducted in the absence of any commercial or financial relationships that could be construed as a potential conflict of interest.

References

- Alocrón Corredor, O., de Fernández, M. R., and Carnevali de Tatá, E. (1998). Los mapas enzimáticos tisulares y séricos y la utilidad diagnóstica de los cocientes enzimáticos: Una revisión. *MedULA* 7, 19–24.
- Aldaba Muruato, L. R., Ventura Juárez, J., Perez Hernandez, A. M., Hernández Morales, A., Muñoz Ortega, M. H., Martínez Hernández, S. L., et al. (2021). Therapeutic perspectives of *p*-coumaric acid: Anti-necrotic, anti-cholestatic and anti-amoebic activities. *World Acad. Sci. J.* 3, 47. doi:10.3892/wasj.2021.118
- Aleksunes, L. M., and Manautou, J. E. (2007). Emerging role of Nrf2 in protecting against hepatic and gastrointestinal disease. *Toxicol. Pathol.* 35 (4), 459–473. doi:10.1080/01926230701311344
- Anlar, H. G. (2020). Cinnamic acid as a dietary antioxidant in diabetes treatment. *Diabetes (Second Edition) Oxidative Stress and Dietary Antioxidants*, 235–243. doi:10.1016/B978-0-12-815776-3.00023-1
- Aranaz, P., Navarro-Herrera, D., Zabala, M., Migueliz, I., Romo-Hualde, A., Lopez-Yoldi, M., et al. (2019). Phenolic compounds inhibit 3T3-L1 adipogenesis depending on the stage of differentiation and their binding affinity to PPAR γ . *Mol. (Basel, Switz.)* 24 (6), 1045. doi:10.3390/molecules24061045
- Bastaki, S., Padol, I. T., Amir, N., and Hunt, R. H. (2018). Effect of Aspirin and ibuprofen either alone or in combination on gastric mucosa and bleeding time and on serum prostaglandin E2 and thromboxane A2 levels in the anaesthetized rats *in vivo*. *Mol. Cell. Biochem.* 438 (1–2), 25–34. doi:10.1007/s11010-017-3110-1
- Battaller, R., and Brenner, D. A. (2005). Liver fibrosis. *J. Clin. Invest.* 115 (2), 209–218. doi:10.1172/JCI24282
- Birch, C. A., Molinar-Inglis, O., and Trejo, J. (2021). Subcellular hot spots of GPCR signaling promote vascular inflammation. *Curr. Opin. Endocr. Metabolic Res.* 16, 37–42. doi:10.1016/j.coemr.2020.07.011
- Cadena-Iníguez, J. (2010). El chayote (*Sechium edule* (Jacq.) Sw., importante recurso fitogenético mesoamericano. *Agro Prod.* 3 (2), 3–10.
- Costet Mejia, A. (2020). Estudio Químico y Actividad Nefroprotectora del Extracto Hidroalcohólico Estandarizado de la Raíz de *Sechium edule* (Jacq sw). Tesis de Maestría. México. Universidad Autónoma del estado de Morelos.
- de insumos de la salud, R (2021). Available at. <http://www.oag.salud.gob.mx/descargas/LV/56-31-05-2021.pdf>.
- Doyon, P., and Servant, M. J. (2010). Tumor necrosis factor receptor-associated factor-6 and ribosomal S6 kinase intracellular pathways link the angiotensin II AT1 receptor to the phosphorylation and activation of the I κ B kinase complex in vascular smooth muscle cells. *J. Biol. Chem.* 285 (40), 30708–30718. doi:10.1074/jbc.M110.126433
- Farmacovigilancia, C. N. (2015). Comisión Federal para la Protección contra Riesgos Sanitarios Obtenido de Comunicado dirigido a los profesionales de la salud ya la población en general: Uso para consumidores de antigripales y medicamentos contra el dolor. *File. C:/Users/rrios/Downloads/COMUNICADO%20PARACETAMOL180215 20* (4).
- Firdous, S., Sravanthi, K., Deb Nath, R., and Neeraja, K. A. (2012). Protective effect of ethanolic extract and its ethylacetate and n-butanol fractions of *Sechium edule* fruits against carbon tetrachloride induced hepatic injury in rats. *Int. J. Pharm. Pharm. Sci.* 4, 354–359.
- Frantz, S., Kelly, R. A., and Bourcier, T. (2001). Role of TLR-2 in the activation of nuclear factor κ B by oxidative stress in cardiac myocytes. *J. Biol. Chem.* 276 (7), 5197–5203. doi:10.1074/jbc.M009160200
- Goldner, J. (1938). A modification of the Masson trichrome technique for routine laboratory purposes. *Am. J. Pathol.* 14, 237–243.
- Gressner, A. M., Weiskirchen, R., Breitkopf, K., and Dooley, S. (2002). Roles of TGF- β in hepatic fibrosis. *Front. Biosci.* 7, A812–d807. doi:10.2741/A812
- Hseu, Y. C., Korivi, M., Lin, F. Y., Li, M. L., Lin, R. W., Wu, J. J., et al. (2018). Trans-cinnamic acid attenuates UVA-induced photoaging through inhibition of AP-1 activation and induction of Nrf2-mediated antioxidant genes in human skin fibroblasts. *J. dermatological Sci.* 90 (2), 123–134. doi:10.1016/j.jdermsci.2018.01.004
- Ibrahim, E. A., Moawed, F., and Moustafa, E. M. (2020). Suppression of inflammatory cascades via novel cinnamic acid nanoparticles in acute hepatitis rat model. *Archives Biochem. biophysics* 696, 108658. doi:10.1016/j.abb.2020.108658
- Karatas, O., Balci Yuce, H., Taskan, M. M., Gevrek, F., Alkan, C., Isiker Kara, G., et al. (2020). Cinnamic acid decreases periodontal inflammation and alveolar bone loss in experimental periodontitis. *J. Periodontol Res.* 55 (5), 676–685. doi:10.1111/jre.12754
- Kawano, Y., and Cohen, D. E. (2013). Mechanisms of hepatic triglyceride accumulation in non-alcoholic fatty liver disease. *J. Gastroenterol.* 48 (4), 434–441. doi:10.1007/s00535-013-0758-5
- Kishida, K., Takeshima, K., Ozaki, Y., and Ihara, H. (2015). The effects of dietary cinnamic acid and *p*-coumaric acid on glucose and lipid metabolism in normal rats fed a high-sucrose diet. *FASEB J.* 29. doi:10.1096/fasebj.29.1_supplement.608.5
- Kishida, K., Suzuki, M., and Ihara, H. (2014). Dietary *p*-coumaric acid modulates hepatic gene expression involved with lipid metabolism in rats (829.6). *FASEB J.* 28. doi:10.1096/fasebj.28.1_supplement.829.6
- Koo, S. H. (2013). Nonalcoholic fatty liver disease: Molecular mechanisms for the hepatic steatosis. *Clin. Mol. Hepatol.* 19 (3), 210–215. doi:10.3350/cmh.2013.19.3.210
- Kopp, C., Singh, S., Regenhard, P., Muller, U., Sauerwein, H., and Mielenz, M. (2014). Trans-cinnamic acid increases adiponectin and the phosphorylation of AMP-activated protein kinase through G-protein-coupled receptor signaling in 3T3-L1 adipocytes. *Int. J. Mol. Sci.* 15, 2906–2915. doi:10.3390/ijms15022906
- Lugo-Baruqui, A., Muñoz-Valle, J. F., Arevalo-Gallegos, S., and Armendariz-Borunda, J. (2010). Role of angiotensin II in liver fibrosis-induced portal hypertension and therapeutic implications. *Hepatology Res. official J. Jpn. Soc. Hepatology* 40 (1), 95–104. doi:10.1111/j.1872-034X.2009.00581.x
- Marion-Letellier, R., Savoye, G., and Ghosh, S. (2016). Fatty acids, eicosanoids and PPAR gamma. *Eur. J. Pharmacol.* 785, 44–49. doi:10.1016/j.ejphar.2015.11.004
- Neog, M. K., Joshua Pragasam, S., Krishnan, M., and Rasool, M. (2017). *p*-Coumaric acid, a dietary polyphenol ameliorates inflammation and curtails cartilage and bone erosion in the rheumatoid arthritis rat model. *BioFactors Oxf. Engl.* 43 (5), 698–717. doi:10.1002/biof.1377

Publisher's note

All claims expressed in this article are solely those of the authors and do not necessarily represent those of their affiliated organizations, or those of the publisher, the editors and the reviewers. Any product that may be evaluated in this article, or claim that may be made by its manufacturer, is not guaranteed or endorsed by the publisher.

Supplementary material

The Supplementary Material for this article can be found online at: <https://www.frontiersin.org/articles/10.3389/fntpr.2022.1043685/full#supplementary-material>

- Nguyen, L. V., Nguyen, K. D. A., Nguyen, Q. T., Nguyen, H. T. H., Yang, D. J., et al. (2021). p-Coumaric acid enhances hypothalamic leptin signaling and glucose homeostasis in mice via differential effects on AMPK activation. *Int. J. Mol. Sci.* 22 (3), 1431. doi:10.3390/ijms22031431
- Nguyen, T., Nioi, P., and Pickett, C. B. (2009). The Nrf2-antioxidant response element signaling pathway and its activation by oxidative stress. *J. Biol. Chem.* 284 (20), 13291–13295. doi:10.1074/jbc.R900010200
- Oseini, A. M., and Sanyal, A. J. (2017). Therapies in non-alcoholic steatohepatitis (NASH). *Liver Int.* 37, 97–103. doi:10.1111/liv.13302
- Paizis, G., Cooper, M. E., Schembri, J. M., Tikellis, C., Burrell, L. M., and Angus, P. W. (2002). Up-regulation of components of the renin-angiotensin system in the bile duct-ligated rat liver. *Gastroenterology* 123 (5), 1667–1676. doi:10.1053/gast.2002.36561
- Patel, S., Rauf, A., Khan, H., and Abu-Izneid, T. (2017). Renin-angiotensin-aldosterone (RAAS): The ubiquitous system for homeostasis and pathologies. *Biomed. Pharmacother.* 94, 317–325. doi:10.1016/j.biopha.2017.07.091
- Polyzos, S. A., Kountouras, J., and Mantzoros, C. S. (2017). Adipose tissue, obesity and non-alcoholic fatty liver disease. *Minerva Endocrinol.* 42 (2), 92–108. doi:10.23736/S0391-1977.16.02563-3
- Rappaport, A. M. (1973). The microcirculatory hepatic unit. *Microvasc. Res.* 6 (2), 212–228. doi:10.1016/0026-2862(73)90021-6
- Rappaport, A. M., and Wilson, W. D. (1958). The structural and functional unit in the human liver (liver acinus). *Anat. Rec. Hob.* 130 (4), 673–689. doi:10.1002/ar.1091300405
- Rolo, A. P., Teodoro, J. S., and Palmeira, C. M. (2012). Role of oxidative stress in the pathogenesis of nonalcoholic steatohepatitis. *Free Radic. Biol. Med.* 52 (1), 59–69. doi:10.1016/j.freeradbiomed.2011.10.003
- Rowe, I. A., Wong, V. W. S., and Loomba, R. (2022). Treatment candidacy for pharmacologic therapies for NASH. *Clin. Gastroenterol. Hepatol.* 20 (6), 1209–1217. doi:10.1016/j.cgh.2021.03.005
- Sabitha, R., Nishi, K., Gunasekaran, V. P., Agilan, B., David, E., Annamalai, G., et al. (2020). p-Coumaric acid attenuates alcohol exposed hepatic injury through MAPKs, apoptosis and Nrf2 signaling in experimental models. *Chemico-biological Interact.* 321, 109044. doi:10.1016/j.cbi.2020.109044
- Sabitha, R., Nishi, K., Gunasekaran, V., Annamalai, G., and Agilan, B. (2019). p-Coumaric acid ameliorates ethanol-induced kidney injury by inhibiting inflammatory cytokine production and NF- κ B signaling in rats. *Asian Pac. J. Trop. Biomed.* 9, 188. doi:10.4103/2221-1691.258998
- Savoia, C., Sada, L., Zezza, L., Pucci, L., Lauri, F. M., Befani, A., et al. (2011). Vascular inflammation and endothelial dysfunction in experimental hypertension. *Int. J. Hypertens.* 2011, 1–8. doi:10.4061/2011/281240
- Schulze, R. J., Schott, M. B., Casey, C. A., Tuma, P. L., and McNiven, M. A. (2019). The cell biology of the hepatocyte: A membrane trafficking machine. *J. Cell Biol.* 218 (7), 2096–2112. doi:10.1083/jcb.201903090
- Schupp, M., Janke, J., Clasen, R., Unger, T., and Kintscher, U. (2004). Angiotensin type 1 receptor blockers induce peroxisome proliferator-activated receptor-gamma activity. *Circulation* 109 (17), 2054–2057. doi:10.1161/01.CIR.0000127955.36250.65
- Schuster, S., Cabrera, D., Arrese, M., and Feldstein, A. E. (2018). Triggering and resolution of inflammation in NASH. *Nat. Rev. Gastroenterol. Hepatol.* 15 (6), 349–364. doi:10.1038/s41575-018-0009-6
- Sekiya, M., Hiraishi, A., Touyama, M., and Sakamoto, K. (2008). Oxidative stress induced lipid accumulation via SREBP1c activation in HepG2 cells. *Biochem. Biophysical Res. Commun.* 375 (4), 602–607. doi:10.1016/j.bbrc.2008.08.068
- Sheka, A. C., Adeyi, O., Thompson, J., Hameed, B., Crawford, P. A., and Ikramuddin, S. (2020). Nonalcoholic steatohepatitis: A review. *JAMA* 323 (12), 1175–1183. doi:10.1001/jama.2020.2298
- Shen, Y., Song, X., Li, L., Sun, J., Jaiswal, Y., Huang, J., et al. (2019). Protective effects of p-coumaric acid against oxidant and hyperlipidemia-an *in vitro* and *in vivo* evaluation. *Biomed. Pharmacother.* 111, 579–587. doi:10.1016/j.biopha.2018.12.074
- Strable, M. S., and Ntambi, J. M. (2010). Genetic control of de novo lipogenesis: Role in diet-induced obesity. *Crit. Rev. Biochem. Mol. Biol.* 45 (3), 199–214. doi:10.3109/10409231003667500
- Sudargo, T., Aulia, B., Prameswari, A. A., Isnansetyo, A., Puspita, I. D., Budiyantri, S. A., et al. (2021). Effect of administration of CHAGURO made of chayote (*Sechium edule*) and tuna (*Thunnus* sp.) on rats induced with streptozotocin-nicotinamide and a high-fat diet. *Curr. Res. Nutr. Food Sci.* 9, 258–266. doi:10.12944/crnfsj.9.1.24
- Sysoeva, V. Y., Ageeva, L. V., Tyurin-Kuzmin, P. A., Sharonov, G. V., Dykanov, D. T., Kalinina, N. I., et al. (2017). Local angiotensin II promotes adipogenic differentiation of human adipose tissue mesenchymal stem cells through type 2 angiotensin receptor. *Stem Cell Res.* 25, 115–122. doi:10.1016/j.scr.2017.10.022
- The Plant List (2013). A working list of all plant species. Available at: www.theplantlist.org.
- Trejo-Moreno, C., Castro-Martinez, G., Mendez-Martinez, M., Jimenez-Ferrer, J. E., Pedraza-Chaverri, J., Arrellin, G., et al. (2018). Acetone fraction from *Sechium edule* (Jacq.) Sw. edible roots exhibits anti-endothelial dysfunction activity. *J. Ethnopharmacol.* 220, 75–86. doi:10.1016/j.jep.2018.02.036
- Trejo-Moreno, C., Jimenez-Ferrer, E., Castro-Martinez, G., Mendez-Martinez, M., Santana, M. A., Arrellin-Rosas, G., et al. (2018). Characterization of a murine model of endothelial dysfunction induced by chronic intraperitoneal administration of angiotensin II. *Sci. Rep.* 11 (1), 21193. doi:10.1038/s41598-021-00676-x
- Uri Flores, A. G. (2021). *Lesión y muerte celular*. Bolivia; Revista De Actualización Clínica Investiga., 2271.
- Wei, Y., Clark, S. E., Morris, E. M., Thyfault, J. P., Uptergrove, G. M., Whaley-Connell, A. T., et al. (2008). Angiotensin II-induced non-alcoholic fatty liver disease is mediated by oxidative stress in transgenic TG(mRen2)27(Ren2) rats. *J. Hepatology* 49 (3), 417–428. doi:10.1016/j.jhep.2008.03.018
- Wu, Y., Wang, M., Yang, T., Qin, L., Hu, Y., Zhao, D., et al. (2021). Cinnamic acid ameliorates nonalcoholic fatty liver disease by suppressing hepatic lipogenesis and promoting fatty acid oxidation. *Evid Based Complement Alternat Med.* 2021, 9561613. doi:10.1155/2021/9561613
- Yamamoto, S., Yancey, P. G., Zuo, Y., Ma, L. J., Kaseda, R., Fogo, A. B., et al. (2011). Macrophage polarization by angiotensin II-type 1 receptor aggravates renal injury-acceleration of atherosclerosis. *Arterioscler. Thromb. Vasc. Biol.* 31 (12), 2856–2864. doi:10.1161/ATVBAHA.111.237198
- Yang, H., Cromley, D., Wang, H., Billheimer, J. T., and Sturley, S. L. (1997). Functional expression of a cDNA to human acyl-coenzyme A:cholesterol acyltransferase in yeast. *J. Biol. Chem.* 272 (7), 3980–3985. doi:10.1074/jbc.272.7.3980
- Yang, M. Y., Chan, K. C., Lee, Y. J., Chang, X. Z., Wu, C. H., and Wang, C. J. (2015). *Sechium edule* shoot extracts and active components improve obesity and a fatty liver that involved reducing hepatic lipogenesis and adipogenesis in high-fat-diet-fed rats. *J. Agric. Food Chem.* 63 (18), 4587–4596. doi:10.1021/acs.jafc.5b00346
- Yoon, S. A., Kang, S. I., Shin, H. S., Kang, S. W., Kim, J. H., Ko, H. C., et al. (2013). p-Coumaric acid modulates glucose and lipid metabolism via AMP-activated protein kinase in L6 skeletal muscle cells. *Biochem. Biophysical Res. Commun.* 432 (4), 553–557. doi:10.1016/j.bbrc.2013.02.067
- Younossi, Z. M., Koenig, A. B., Abdelatif, D., Fazel, Y., Henry, L., and Wymers, M. (2016). Global epidemiology of nonalcoholic fatty liver disease-Meta-analytic assessment of prevalence, incidence, and outcomes. *Hepatology* 64 (1), 73–84. doi:10.1002/hep.28431